

1 **Dissolved organic matter produced by *Thalassiosira pseudonana***

2 Krista Longnecker, Melissa C. Kido Soule, and Elizabeth B. Kujawinski\*.

3 Woods Hole Oceanographic Institution, Marine Chemistry and Geochemistry, Woods Hole, MA  
4 02543, U.S.A.

5 For submission to: *Marine Chemistry*

6 Date submitted: March 11, 2014 ; 1<sup>st</sup> revised version submitted September 10, 2014, 2<sup>nd</sup> revision  
7 submitted October 28, 2014

8 Running title: Phytoplankton metabolomics

9 \*Corresponding author. Mailing address: WHOI MS#4, Woods Hole, MA 02543. Phone: (508)  
10 289-3493. Fax: (508) 457-2164. E-mail: [ekujawinski@whoi.edu](mailto:ekujawinski@whoi.edu)

11 Keywords: metabolomics, marine phytoplankton, dissolved organic matter

12

13 **Abstract**

14           Phytoplankton are significant producers of dissolved organic matter (DOM) in marine  
15 ecosystems but the identity and dynamics of this DOM remain poorly constrained. Knowledge  
16 on the identity and dynamics of DOM are crucial for understanding the molecular-level reactions  
17 at the base of the global carbon cycle. Here we apply emerging analytical and computational  
18 tools from metabolomics to investigate the composition of DOM produced by the centric diatom  
19 *Thalassiosira pseudonana*. We assessed both intracellular metabolites within *T. pseudonana* (the  
20 endo-metabolome) and extracellular metabolites released by *T. pseudonana* (the exo-  
21 metabolome). The intracellular metabolites had a more variable composition than the  
22 extracellular metabolites. We putatively identified novel compounds not previously associated  
23 with *T. pseudonana* as well as compounds that have previously been identified within *T.*  
24 *pseudonana*'s metabolic capacity (e.g. dimethylsulfoniopropionate and degradation products of  
25 chitin). The resulting information will provide the basis for future experiments to assess the  
26 impact of *T. pseudonana* on the composition of dissolved organic matter in marine  
27 environments.

## 28 1 Introduction

29 Autotrophic microbes play a central role in the global carbon cycle because they fix  
30 inorganic carbon into organic compounds. A fraction of this organic material is released into the  
31 surrounding environment as dissolved organic matter (DOM), where it supports microbial  
32 growth or is respired to carbon dioxide (del Giorgio and Cole, 1998; Kirchman, 2008). The rates  
33 of utilization or remineralization of individual compounds are determined by their structure,  
34 concentration, and the metabolic properties of ambient microorganisms (Azam and Worden,  
35 2004). Thus, the molecular-level composition of DOM is an important factor in our  
36 understanding of the global carbon cycle. Despite the significance of photosynthesis in the  
37 production of organic matter, we know little about the molecular-level composition of  
38 photosynthetically-derived DOM and the environmental factors that govern its production  
39 (reviewed in: Carlson, 2002; Kujawinski, 2011).

40 Centric and pennate diatoms bloom in both coastal and open ocean settings where up to  
41 40% of carbon fixation in marine ecosystems is attributed to these organisms (Nelson et al.,  
42 1995; Tréguer et al., 1995). The centric diatom *Thalassiosira pseudonana* has received  
43 significant attention as a laboratory model organism (Bowler et al., 2010). It was the first diatom  
44 with a completed genome, although function could only be determined for half of the genes  
45 (Armbrust et al., 2004). More recently, there have been genomic, transcriptomic, and proteomic  
46 investigations of *T. pseudonana* which have revealed dynamic responses to growth state, light,  
47 and nutrients (Dyhrman et al., 2012; Montsant et al., 2007; Norden-Krichmar et al., 2011; Nunn  
48 et al., 2009; Shi et al., 2013). Yet our knowledge of *T. pseudonana*'s impact on the composition  
49 of organic matter in marine environments has not been well-explored.

50 Metabolomics is an emerging analytical approach that seeks to characterize metabolites  
51 produced by an organism during growth or released following cell death. In targeted  
52 metabolomics, a limited set of known metabolites is quantified as a function of the process under  
53 study. In contrast, untargeted metabolomics investigations (e.g., Böttcher et al., 2008; Long et  
54 al., 2011) have no pre-defined list of metabolites and use qualitative, or semi-quantitative, mass  
55 spectrometry to examine all possible features. Untargeted metabolomics datasets are immense  
56 with thousands of resolved features, and informatics and statistical tools are employed to identify  
57 the subset of biologically relevant compounds (Patti et al., 2012). Although complete  
58 characterization is not feasible with available analytical methodologies, practitioners have used  
59 electrospray ionization (ESI) mass spectrometry (MS) and nuclear magnetic resonance  
60 spectrometry (NMR) to resolve and identify important molecules within plant systems (Iijima et  
61 al., 2008; Quanbeck et al., 2012) and within model microorganisms such as *Escherichia coli*  
62 (Rabinowitz and Kimball, 2007). These projects have provided valuable information on method  
63 development and computational tools which have allowed detailed examinations of the chemical  
64 interactions between biological entities and their habitats.

65 In the marine ecosystem, metabolic assessments of microorganisms have focused on  
66 phytoplankton such as cyanobacteria (Baran et al., 2010; Bennette et al., 2011) and diatoms (Paul  
67 et al., 2009). Experiments with these microbes have revealed that variability in phytoplankton-  
68 derived metabolites can be linked to growth stage (Barofsky et al., 2009; Vidoudez and Pohnert,  
69 2012), nutrient limitation (Bromke et al., 2013), and are affected by the presence of co-cultured  
70 phytoplankton (Paul et al., 2009). Although recovery of targeted compounds has been used to  
71 optimize metabolite extraction and analysis methods (Bennette et al., 2011), structural  
72 characterization and identification of most metabolites remains challenging (Baran et al., 2010).

73           The goal of this project was an exploration of the molecular-level composition of  
74 metabolites produced by an autotrophic microorganism in order to characterize the metabolites  
75 released into the marine environment as a result of photoautotrophic processes. We extracted  
76 intracellular and extracellular metabolites from a laboratory culture of *T. pseudonana* and  
77 examined their composition over time with liquid chromatography coupled to ultrahigh  
78 resolution mass spectrometry (LC/FT-ICR-MS). Our analysis confirmed the presence of  
79 metabolites previously identified as part of *T. pseudonana*'s metabolic capacity as well as  
80 specific metabolites not previously known to occur in *T. pseudonana*.

## 81 **2 Experimental section**

### 82 **2.1 Culturing *Thalassiosira pseudonana***

83           The diatom *Thalassiosira pseudonana* (CCMP culture #1335) was cultured axenically in  
84 a modified version of L1 media made with an artificial salt solution (Turks Island Salts) with  
85 extra silicate ( $212 \mu\text{mol L}^{-1}$ ) and  $10 \mu\text{mol L}^{-1}$  selenous acid. The cultures were initiated by  
86 adding 30 ml of *T. pseudonana* in exponential growth to twelve flasks with an additional six  
87 flasks serving as cell-free controls; each flask initially contained 300 ml of media. The cultures  
88 were incubated at  $12^\circ\text{C}$  under a 12h:12h light:dark cycle. Samples were collected six hours into  
89 the light cycle on days 0, 1, 3, 7, 8, and 10. Three flasks were destructively sampled at each time:  
90 two replicates with *T. pseudonana* and one cell-free control. In order to characterize the temporal  
91 variability in DOM and include cell-free controls, we could not accommodate more than two  
92 replicates with *T. pseudonana* and the cell-free control for each time point.

### 93 **2.2 Ancillary samples**

94           At each time point, sample aliquots were removed for total organic carbon and nutrient  
95 analyses, and for cell counts. Unfiltered water samples for total organic carbon were acidified to

96 pH = 2 with 12 M hydrochloric acid, and stored at 4°C until analysis on a Shimadzu TOC-V<sub>CSH</sub>  
97 total organic carbon analyzer. The coefficient of variability between replicate injections was  
98 <1%. Comparisons to standards provided by Prof. D. Hansell (University of Miami) were made  
99 daily to verify that the measured concentrations of the standard fell within the consensus values  
100 for total organic carbon. The unfiltered water samples were also used to obtain concentrations of  
101 nitrate + nitrite, ammonium, silicate, and phosphate using a Lachat Instruments QuickChem  
102 8000 continuous flow injection system. For cell counts, samples were fixed with 10%  
103 formaldehyde (final concentration) and stored at -80°C until cells were counted using a Reichert  
104 hemocytometer. The formaldehyde-fixed cells were also stained with DAPI and viewed with an  
105 epifluorescence microscope to check for potential contamination by heterotrophic  
106 microorganisms. Contamination was not observed at any time point during the experiment.

### 107 **2.3 Extraction of metabolites**

108 Our initial experiments testing different extraction and mass spectrometry methods  
109 showed that extraction protocols appropriate for freshwater microorganisms such as a  
110 methanol/chloroform extraction (Winder et al., 2008) cannot be readily applied to marine  
111 organisms. The salt in seawater and the growth media is problematic for ESI mass spectrometry  
112 because salt suppresses the ionization of the organic molecules. For this reason, we were not able  
113 to analyze intracellular metabolites by direct infusion into the mass spectrometer. Rather, for  
114 both intracellular and extracellular metabolites, we opted for a reversed-phase LC/FT-MS  
115 method, in which salt co-elutes with the solvent front and is removed from compounds that are  
116 retained on the chromatography column. We adapted existing extraction and analysis methods to  
117 distinguish the organic compounds produced by *T. pseudonana* from the organic compounds in

118 the growth media. The methods for extracting intracellular and extracellular metabolites  
119 proceeded identically for the flasks with *T. pseudonana* and the cell-free controls.

120 The intracellular metabolites were extracted using a method developed by Rabinowitz  
121 and Kimball (2007). Briefly, 1.5 ml samples were centrifuged at 16,000 x g at 4°C for 30 minutes  
122 and the supernatant discarded. The resulting cell pellet was extracted three times with ice-cold  
123 extraction solvent (acetonitrile:methanol:water with 0.1 M formic acid, 40:40:20). The combined  
124 extracts were neutralized with 0.1 M ammonium hydroxide, dried in a vacufuge, and then re-  
125 dissolved in 1 mL of 90:10 (v/v) water:acetonitrile for analysis on the mass spectrometer.

126 Prior to sampling the extracellular metabolites, the cells were removed by gentle vacuum  
127 filtration through 0.2 µm Omnipore filters (hydrophilic PTFE membranes, Millipore). Barofsky  
128 et al. (2009) have observed filtration may release intracellular metabolites into the  
129 exometabolome, and this potential bias must be considered in the discussion of our results. The  
130 acidified filtrate was extracted using solid phase extraction with PPL cartridges (Varian Bond  
131 Elut PPL cartridges) as previously described (Dittmar et al., 2008). After eluting with methanol,  
132 the extracts were dried in a vacufuge, and then re-dissolved in 1 mL 90:10 water:acetonitrile  
133 prior to analysis.

134 We quantified the extraction efficiency of the solid phase extraction resin in the  
135 following manner. The water:acetonitrile solution was dried completely using a vacufuge and re-  
136 dissolved in MilliQ water. The extract was then added to MilliQ water that had been acidified  
137 with hydrochloric acid and analyzed on a Shimadzu TOC-V<sub>CSH</sub> total organic carbon analyzer as  
138 described in section 2.2. The carbon concentration from the extract was compared to the  
139 concentration of dissolved organic carbon in the filtrate to calculate the percent of organic carbon  
140 retained by the PPL cartridges.

## 141 **2.4 Analysis of metabolites**

142 All metabolomics analyses were conducted using liquid chromatography (LC) coupled by  
143 electrospray ionization to a hybrid linear ion trap - Fourier-transform ion cyclotron resonance  
144 (FT-ICR) mass spectrometer (7T LTQ FT Ultra, Thermo Scientific). Samples were stored at  
145 -20°C until mass spectrometric analysis. Analysis of the extracts was conducted within 48 hours  
146 of sample processing, except for the extracts from day three which were analyzed six days after  
147 sample processing. LC separation was performed on a Synergi Fusion reversed-phase column  
148 using a binary gradient with solvent A being water with 0.1% formic acid and solvent B being  
149 acetonitrile with 0.1% formic acid. Samples were eluted at 250  $\mu\text{l min}^{-1}$  with the following  
150 gradient: hold at 5% B for 0-2 min, ramp from 5 to 65% B between 2 and 20 min, ramp from 65  
151 to 100% B between 20 and 25 min, hold at 100% B from 25-32 min, and then ramp back to 5%  
152 B between 32 and 32.5 min for re-equilibration (32.5-40 min). Both full MS and MS/MS data  
153 were collected. The MS scan was performed in the FT- ICR cell from  $m/z$  100-1000 at 100,000  
154 resolving power (defined at 400  $m/z$ ). In parallel to the FT acquisition, MS/MS scans were  
155 collected at nominal mass resolution in the ion trap from the two features with the highest peak  
156 intensities in each scan. Separate autosampler injections were made for analysis in positive and  
157 negative ion modes.

158 Electrospray and mass spectrometry conditions were initially optimized by infusing a  
159 mixture of metabolite standards in positive and negative ion modes. The list of compounds  
160 within this solution and sample spectra are given in Fig.S1. The majority of these standards  
161 preferentially ionize in either positive or negative ion mode. The LTQ FT Ultra was also  
162 externally calibrated weekly using a standard mixture of caffeine (Sigma Aldrich), L-methionyl-  
163 arginyl-phenylalanyl-alanine acetate (MRFA) (Sigma Aldrich), Ultramark 1621 (Alfa Aesar),



164 acetic acid (Sigma Aldrich), sodium dodecyl sulfate (Sigma Aldrich), and sodium taurocholate  
165 (Sigma Aldrich). The instrument has a mass accuracy of < 2 ppm after external calibration.

## 166 **2.5 Processing of mass spectral data and feature identification**

167 Data were collected as XCalibur RAW files which were converted to mzXML files using  
168 the msConvert tool within ProteoWizard (Chambers et al., 2012). Features were extracted from  
169 the LC-MS data using XCMS (Smith et al., 2006), where a feature is defined as a unique  
170 combination of a mass-to-charge ( $m/z$ ) ratio and a retention time. Peak finding was performed  
171 with the centWave algorithm (Tautenhahn et al., 2008), and only peaks that fit a Gaussian shape  
172 were retained. Features were aligned across samples based on retention time and  $m/z$  value using  
173 the group.nearest function in XCMS; fillPeaks was used to reconsider features missed in the  
174 initial peak finding steps. CAMERA was used (1) to find compounds differing by adduct ion and  
175 stable isotope composition (Kuhl et al., 2012) and (2) to extract the intensities and  $m/z$  values for  
176 the associated MS/MS spectra. Finally, the list of features with their retention time,  $m/z$  value,  
177 and intensity from the extracted ion chromatographs (EIC peak heights) were exported to  
178 MATLAB for further processing. Positive and negative ion mode data were processed as  
179 separate datasets in XCMS and MATLAB.

180 In order to compare the data from the LC-based analysis with analyses generally done for  
181 direct infusion ESI FT-ICR MS data, we calculated the elemental formulas for the  $m/z$  values  
182 from the mzXML files processed by XCMS. We used the Compound Identification Algorithm  
183 developed by Kujawinski and colleagues (Kujawinski and Behn, 2006; Kujawinski et al., 2009)  
184 with a formula error of 1 ppm, and a relationship error of 20 ppm. The mass limit above which  
185 elemental formulas were assigned only by functional group relationships was 500 Da. Elements  
186 considered are C, H, O, N, S, and P. These elemental formulas were then divided into compound

187 classes that have been defined based on elemental ratios as approximated from data within  
188 Hedges and Kim et al. (Hedges, 1990; Kim et al., 2003).

189 Several databases and *in silico* tools were consulted in order to make putative  
190 identifications of select features from the untargeted metabolomics data. The databases included  
191 the Madison Metabolomics Consortium Database (MMCD, Cui et al., 2008), METLIN (Smith et  
192 al., 2005), and to a lesser extent MassBank (Horai et al., 2010), PubChem, and KEGG. The  
193 database searches described in the present project allowed a 2 ppm window between the  
194 measured and the database (calculated)  $m/z$  values.

## 195 **2.6 Statistical analysis**

196 Non-metric multidimensional scaling (NMS) (Kruskal, 1964; Mather, 1976) was used to  
197 analyze variability in metabolite composition. For this analysis, only the compounds that were  
198 not found in the controls were considered; the list was not pruned to remove isotopologues or  
199 adducts. Differences between individual samples were calculated based on the presence or  
200 absence of features with the Bray-Curtis distance measure using the Fathom toolbox (D.L. Jones,  
201 pers. comm.). The statistics toolbox in MATLAB was used to run the NMS analyses. The  
202 dimensionality of the data set was assessed by comparing 40 runs with real data to 50 runs with  
203 randomized data. Additional axes were considered if the addition of the axis resulted in a  
204 significant improvement over the randomized data (at  $p \leq 0.05$ ) and the reduction in stress was  
205 greater than 0.05. Stress is a metric of goodness of fit in NMS data, and thus large reductions in  
206 stress indicate that the additional axis significantly improved the presentation of the data. The  
207 proportion of variation represented by each axis was assessed by using a Mantel test to calculate  
208 the coefficient of determination ( $r^2$ ) between distance in the ordination space and distance in the  
209 original space.

210 Model I regressions were used to quantify changes in EIC peak heights during the  
211 experiment. The non-parametric Spearman's rank correlation implemented in MATLAB was  
212 used to test changes in compound classes, cell abundance, TOC concentration, and inorganic  
213 nitrogen concentrations during the experiment.

## 214 **3 Results and Discussion**

### 215 **3.1 Using metabolomics to assess the impact of an organism on its chemical** 216 **environment**

217 Metabolomics seeks to describe and quantify metabolites produced by organisms in  
218 response to their chemical microenvironment (Patti et al., 2012). To address this goal for the  
219 centric diatom, *T. pseudonana*, we analyzed our untargeted metabolomics data in two ways.  
220 First, we consider the pattern of shared metabolites in order to examine the similarities (or  
221 differences) between samples or along a time series. These comparisons do not require  
222 identification of unknown compounds; rather all detected intracellular and extracellular  
223 metabolites can be compared over time. Second, the list of  $m/z$  values was mined to obtain  
224 putative compound identifications. While there is still need for increased coverage of  
225 metabolomics databases (Kind et al., 2009), obtaining the identity of a compound greatly  
226 expands our ability to understand the chemical impact of microbes such as diatoms. For example,  
227 with a compound identification we can consider the environmental conditions that affect the  
228 concentration of a metabolite, describe the biochemical pathways in which it occurs, and  
229 examine the sources and sinks of this compound in the environment. This remains a major  
230 challenge in environmental metabolomics, and is one that cannot be achieved solely within the  
231 context of our work with *T. pseudonana*. In the following sections, we discuss the pattern of

232 compounds produced by *T. pseudonana* and then the compounds that we were able to putatively  
233 identify.

### 234 **3.2 Temporal patterns in *T. pseudonana* metabolites**

235 Over the course of the ten-day experiment, there were significant increases in the  
236 abundance of *T. pseudonana* and the concentration of total organic carbon concurrent with  
237 significant decreases in the inorganic nutrient concentrations (Spearman rank correlations, p-  
238 values all  $\ll 0.0001$ , Fig. S2). The inoculum into the flasks with *T. pseudonana* resulted in the  
239 transfer of organic compounds into the flasks at the beginning of this experiment as is apparent  
240 in the higher total organic carbon concentrations observed at the first sampling point in the flasks  
241 with *T. pseudonana* compared to the cell-free controls (Fig. S2). The cell-free controls did not  
242 show statistically significant changes over time in cell abundance, TOC, or inorganic nutrient  
243 concentrations (Spearman rank correlations, p-values  $> 0.05$ ).

244 We use two measures to compare our extracellular extracts with previous research on  
245 dissolved organic matter. First, we consider the fraction of dissolved organic carbon that was  
246 recovered with solid phase extraction. We recovered between 14 and 41% of the organic  
247 compounds with the PPL cartridges, with increased extraction efficiencies at the later growth  
248 stages of the experiment (Fig. 1). By comparison, Becker et al. (2014) recovered between 2 and  
249 24% of dissolved organic carbon from their phytoplankton cultures, with variability in the  
250 extraction efficiency correlated to phytoplankton phylogeny. Both studies observe efficiencies  
251 below the 40-60% extraction efficiency measured by Dittmar et al. (2008) for water samples  
252 from marine and estuarine sites. Second,  $m/z$  values from ultrahigh resolution mass spectrometry  
253 data have previously been sorted into compound classes based on their elemental ratios (e.g.,  
254 Bhatia et al., 2010; Minor et al., 2012). Using this approach, the DOM from *T. pseudonana*

255 contains primarily protein-like, condensed hydrocarbon-like, and lipid-like compounds (Fig. 2);  
256 with lignin-like and carbohydrate-like compounds comprising less than 1% of the assigned  
257 elemental formulas. However, only a small fraction of the DOM could be sorted into compound  
258 classes based on elemental formulas. The proteins, hydrocarbons, and lipids from the positive ion  
259 mode data showed statistically significant increases with time; in negative ion mode, only the  
260 correlation between proteins and sampling time was statistically significant (Spearman's rho, p-  
261 values <0.05). While these compound classes do not distinguish between structural isomers, they  
262 provide a means to compare the composition of different samples. Here, we show that increases  
263 in *T. pseudonana* abundance are linked to higher numbers of protein-like, condensed  
264 hydrocarbon-like, and lipid-like compounds. These broad classifications, however, also highlight  
265 the limitations of analyses based on elemental formulas, which cannot distinguish between  
266 structural isomers. As we will note in section 3.4, we observed instances of the same  $m/z$  value at  
267 different retention times, confirming the presence of structural isomers in this dataset.

268         The number of features detected within the sample extracts analyzed with our untargeted  
269 metabolomics method showed slight variability during the course of the experiment (Table 1,  
270 Fig. S3). The data summarized in Table 1 includes all unique combinations of an  $m/z$  value and a  
271 retention time; specific compounds will appear in this list multiple times if they were observed  
272 with different adducts (e.g.,  $M-H^+$  or  $M-Na^+$ ) or with  $^{13}C$  substitutions (i.e., isotopologues).  
273 Almost 75% of all features were observed only in the treatments with *T. pseudonana* and were  
274 absent in the cell-free controls. The features found both in the treatments with *T. pseudonana* and  
275 in the cell-free controls were not analyzed further.

276         Throughout the experiment, we detected more features in the exometabolome compared  
277 to the endometabolome in both positive and negative ion modes (Fig. S3). There are several

278 factors that contribute to this observation. First, a smaller volume of sample was processed to  
279 obtain the intracellular metabolites. Thus, metabolites present at lower concentrations may not  
280 have sufficient signal strength to be detected by the mass spectrometer. Second, methodological  
281 constraints required us to use a different extraction method to assess the endometabolome  
282 compared to the exometabolome. This might have affected the number and type of features  
283 retained and likely impacted the patterns of features observed within the intracellular and  
284 extracellular metabolite pools. The primary goal of extraction methods for both intra- and  
285 extracellular metabolites is the capture of the broadest suite of compounds at sufficient  
286 concentration and with minimal salt interference. Due to the different sample matrices, this  
287 requires two different extraction methods. In the intracellular methods, simple cell lysis liberates  
288 a diverse pool of compounds and salt removal occurs during the LC step. For extracellular  
289 methods, compounds must be concentrated from the saltwater media, requiring the use of solid-  
290 phase extraction resins. De-salting occurs at the same time as extraction in this method. The  
291 method for the intracellular metabolites is optimal for low molecular weight compounds that are  
292 more polar compared to the slightly less polar, moderate molecular weight compounds which are  
293 captured by the PPL solid-phase extraction cartridges used for the extracellular metabolites.  
294 Nevertheless the boundaries of polarity and molecular weight are not exclusive to each method,  
295 and we expected overlap in the compounds observed in the intracellular and extracellular  
296 metabolites extracted from *T. pseudonana*. Yet, only a small number of compounds (9 in  
297 negative ion mode and 35 in positive ion mode) from *T. pseudonana* were observed in both the  
298 intracellular and extracellular metabolites (Table 1). Whether or not this was due to changes in  
299 the metabolites after they were exuded from the cells cannot be determined based on our current  
300 data. Previous research has noted that filtration of diatom cells may cause intracellular

301 metabolites to leak from cells which would bias characterization of extracellular metabolites  
302 (Barofsky et al., 2009). Of the limited research that has been done into metabolites of marine  
303 microorganisms, only two studies that we are aware of have attempted to examine both  
304 intracellular and extracellular metabolites (Baran et al., 2010; Rosselló-Mora et al., 2008), and  
305 neither of these studies assessed the overlap between the intracellular and extracellular  
306 metabolites in their organisms.

307         Changes in the extracted-ion-current (EIC) peak heights can be a semi-quantitative  
308 measure of the amount of a feature within a sample. EIC peak heights may vary because of (1)  
309 variability in the mass spectrometer, (2) ionization efficiency of the different compounds, and (3)  
310 the concentration of a compound within a sample. By definition, the present project took a finite  
311 amount of time and we opted to analyze the samples a constant length of time after extraction in  
312 order to minimize changes to the extract. This precludes analysis of the samples in a randomized  
313 fashion, which would reduce the impact of instrument variability. An alternative option is to  
314 group the sample extractions required for one project. This allows a pooled sample to be created  
315 which can constrain differences in EIC peak heights that are due to analytical variability (Dunn  
316 et al., 2011). Almost 9,000 features were observed in positive and negative ion mode and absent  
317 from the cell-free controls (Table 1, Fig. S3). A fraction of these features showed significant  
318 increases or decreases in EIC peak heights over the experiment (Table S1). More of the  
319 extracellular metabolites showed increases in EIC peak heights over time compared to the  
320 intracellular metabolites in both positive and negative ion modes (Table S1). Furthermore, a  
321 higher percentage of features decreased over time in the extracellular compared to the  
322 intracellular metabolites (Table S1). Such temporal variability over different growth stages in  
323 extracellular metabolites released by *T. pseudonana* has also been noted by Barofsky et al.

324 (2009). Yet, when all samples over the six sampling days were considered, the majority of  
325 features did not exhibit statistically significant changes in EIC peak heights during the  
326 experiment. The metabolites not exhibiting temporal variability could be compounds replenished  
327 by *T. pseudonana* at a constant rate or compounds that are not affected by changes in the growth  
328 conditions of the present project. While we cannot exclude the possibility that a subset of these  
329 metabolites were transferred with the inoculum at the beginning of the experiment, these features  
330 were absent from the controls and therefore not present in the media used to grow *T.*  
331 *pseudonana*.

### 332 **3.3 Statistical analysis of occurrence patterns of metabolites**

333 We used NMS to analyze the pattern of features found in the intracellular and  
334 extracellular metabolites. In positive ion mode, the NMS calculation (Fig. 3A and B) resulted in  
335 an ordination with a final stress of 0.13 and  $r^2 = 0.89$  with more variability on axis one than on  
336 axis two ( $r^2$  on axis 1 = 0.66,  $r^2$  on axis 2 = 0.32). In negative ion mode, the NMS calculation  
337 (Fig. 3C and D) resulted in an ordination with a final stress of 0.12 and  $r^2 = 0.78$  with more  
338 variability on axis one than on axis two ( $r^2$  on axis 1 = 0.57,  $r^2$  on axis 2 = 0.20). In both positive  
339 and negative ion modes, the NMS revealed a larger variability in the intracellular metabolites  
340 compared to the variability in the extracellular metabolites. In negative ion mode, this pattern  
341 was predominantly due to differences observed in one replicate on days 1, 8, and 10. This  
342 variability between replicates sampled on days 1, 8, and 10 was also evident in positive ion  
343 mode. We do not have an explanation for this inter-replicate variability for select days of the  
344 experiment, but the fact that it was observed in both positive and negative ion modes suggests  
345 either variability in biological activity or sample processing, and not analytical variability. The  
346 positive ion mode data exhibited greater differences among samples collected at all of the time



347 points. By day 7 of the experiment, the NMS revealed small changes in the composition of  
348 extracellular metabolites as shown by the tight clustering of symbols for days 7, 8, and 10 in Fig.  
349 3. This indicates that the composition of metabolites produced by *T. pseudonana* at the  
350 conclusion of the experiment was less dynamic and fewer new compounds were being produced  
351 compared to the more variable composition of metabolites observed during exponential growth.

### 352 **3.4 Annotating metabolites from *T. pseudonana***

353 A major challenge with an untargeted metabolomics assessment is the task of fully  
354 identifying the tens of thousands of features detected within a single dataset (Daly et al., 2014;  
355 Schymanski and Neumann, 2013). In the ideal case, these identifications are validated using  
356 authentic standards and multiple analytical methods coupled to iterative comparisons to different  
357 databases (Sumner et al., 2007). This labor-intensive process currently renders identification of  
358 the ~18,000 features found in the present project (Table 1) infeasible. Therefore, we culled our  
359 dataset to focus attention on those compounds that would have the highest potential for  
360 significant interest. To address our scientific goal of identifying compounds produced by *T.*  
361 *pseudonana* and subsequently released into the environment, we focused our attention on  
362 features detected in both intracellular and extracellular extracts. As described in the methods  
363 section, we required a feature (a) to be absent from the cell-free controls, and additionally  
364 required features (b) to be present in both replicates with *T. pseudonana* in order to increase our  
365 confidence in the observation of each feature, and (c) to be present at more than one time point in  
366 order to avoid considering transient features within the dataset. In the end, nine compounds in  
367 negative ion mode and 35 compounds in positive ion mode (Table 1) met these stringent criteria  
368 and we attempted to identify them based on exact mass and MS/MS data.

369 We used an iterative process to annotate and putatively identify the compounds, with  
370 comparisons to multiple databases. We used a classification scheme proposed by Sumner et al.  
371 (2007) to rate the strength of our putative metabolite identifications (Table 2). The strongest  
372 identifications, level 1, are those for which we have an authentic standard and have analyzed it  
373 on our mass spectrometer. Level 2 identifications are putatively annotated without chemical  
374 reference standards, but are based on spectral similarities with data from public or commercial  
375 libraries. Compounds with only a match based on  $m/z$  value are rated as level 3 classifications  
376 within the Sumner et al. (2007) format. Finally, level 4 classifications are unknown compounds.  
377 Searches based on comparisons of exact mass and the KEGG database have been previously  
378 used to help characterize organic compounds (Longnecker and Kujawinski, 2011; Romano et al.,  
379 2014; Suhre and Schmitt-Kopplin, 2008). Here, our first step in identification was comparison of  
380 exact mass values with masses of metabolites present in METLIN. In addition, for features with  
381 MS/MS fragmentation in our experiment, we compared our MS/MS spectra with METLIN  
382 database spectra to assign a putative identification to the feature. However, not all compounds in  
383 the METLIN database have associated MS/MS spectra. When no MS/MS data or matches to the  
384 METLIN database were available for a selected feature, we consulted the MMCD database.  
385 Finally, four of the features in positive ion mode were eliminated from consideration because the  
386 features had the same  $m/z$  value with different retention times, suggesting the presence of  
387 structural isomers. Identifying these features would require analysis of authentic standards of  
388 possible isomers to establish appropriate retention times and MS/MS data for comparison with  
389 our experimental dataset. In the following sections we discuss the implications of the compounds  
390 we were able to putatively identify (Table 2, Table S2).

### 391 **3.5 Observation of compounds previously associated with *T. pseudonana***

392 Chitin is produced by a variety of marine organisms, and crustacean shells are the largest  
393 pool of chitin in the marine environment. After cellulose, chitin is the second most abundant  
394 biopolymer on earth yet its low levels in marine sediments imply that it is readily recycled within  
395 marine ecosystems despite its poor aqueous solubility (Gooday, 1990; Jeuniaux and Voss-  
396 Foucart, 1991). In *T. pseudonana*, the chitin is found in the cell wall (Brunner et al., 2009;  
397 Durkin et al., 2009) and flexible chitin fibers extend through the silica channels surrounding the  
398 cell (Hildebrand et al., 2009). In the present project, we observed both tri-N-acetylchitotriose  
399 (Fig. 4A) and chitobiose, which corroborates previous observations from culture experiments  
400 with *T. pseudonana* (Smucker and Dawson, 1986). The extracted ion chromatogram of tri-N-  
401 acetylchitotriose is shown in Fig. S4. The putative identification of tri-N-acetylchitotriose was  
402 well supported because the METLIN database provided a match for its exact mass and a match  
403 for the measured MS/MS spectra (Fig. 4B). Furthermore, the retention time for an authentic  
404 standard matched the retention time measured in the culture experiment. The *T. pseudonana*  
405 genome contains the synthetic pathway for chitin and 22 putative chitinases, which have a  
406 potential for chitin degradation (Armbrust et al., 2004). One hypothesis is that *T. pseudonana*  
407 degrades chitin to alter its sinking rate or to change the thickness of its cell wall to modulate the  
408 influx of compounds (Armbrust et al., 2004). An alternate hypothesis is that *T. pseudonana* does  
409 not express its chitinases for chitin degradation and that tri-N-acetylchitotriose and chitobiose are  
410 lost from chitin fibers during cellular growth. This hypothesis is consistent with culture  
411 experiments that did not reveal measurable levels of chitinase activity under different growth  
412 conditions (Štrojsová and Dyrhman, 2008). However, this would not explain the presence of  
413 multiple chitinases within the *T. pseudonana* genome. While we cannot distinguish between

414 these two hypotheses with the present dataset, the observed increases in tri-N-acetylchitotriose  
415 and possibly chitobiose suggest that the metabolic potential for chitin degradation in the genome  
416 could be realized during the growth of *T. pseudonana*. This is a good example of a case where  
417 genomic data are helpful in describing potential microbial metabolisms, yet metabolomics data  
418 are required to quantify the actual metabolic processes active within marine environments.

419         As the experiment progressed, *Thalassiosira* retained increasing amounts of intracellular  
420 dimethylsulfoniopropionate (DMSP; Fig. S5). DMSP was identified by exact *m/z* matches in the  
421 MMCD database and through analysis of an authentic standard. The identification of DMSP also  
422 indicates that we were able to distinguish chemical compounds that are important in marine  
423 environments, even with an untargeted metabolomics approach. DMSP is an organic sulfur  
424 compound that can act as an osmolyte for marine phytoplankton (Kirst, 1990). In addition,  
425 internal DMSP might scavenge potentially damaging reactive oxygen species or serve as a sink  
426 for carbon during periods of unbalanced growth (Stefels et al., 2007). In *T. pseudonana*, the  
427 production of DMSP is well-established (Keller et al., 1999) and increased amounts of DMSP  
428 are produced when the cells are nitrogen-limited (Bromke et al., 2013; Bucciarelli and Sunda,  
429 2003; Franklin et al., 2012). In the present project, we did not add DSMP to the media and we  
430 did not detect DMSP in the cell-free controls. Yet, the amount of DMSP inside the cells  
431 increased during the experiment which might reflect *T. pseudonana*'s response to decreasing  
432 nitrogen availability, although the concentration of inorganic nitrogen always remained above  
433 600  $\mu$ M during the experiment (Fig. S2). While DMSP was observed at low levels in the external  
434 metabolites, DMSP is not efficiently recovered by PPL cartridges and thus its detection in this  
435 pool was likely underestimated significantly (W. Johnson, personal communication). The  
436 amount of DMSP produced by different species of phytoplankton varies over several orders of

437 magnitude, with diatoms having lower DMSP-to-carbon ratios than other phytoplankton (Stefels  
438 et al., 2007). However, our observation and the recent observations by Franklin et al. (2012)  
439 indicate that *Thalassiosira* may be important in the production of DMSP and therefore plays a  
440 role within the marine sulfur cycle.

### 441 **3.6 Identification of compounds not previously associated with *T. pseudonana***

442 Compound identification is a major challenge in environmental metabolomics. In the  
443 following discussion, we present putatively annotated features, but recognize that there is still  
444 uncertainty associated with these identifications. Thus, a definitive identification will require  
445 additional verification before we can hypothesize as to the role of these compounds within the  
446 metabolism of *T. pseudonana*. Once we have confirmed the identity of these compounds, we can  
447 develop an appropriate quantitative assay and conduct laboratory experiments to address  
448 hypotheses about the importance of these compounds in the chemical ecology of *T. pseudonana*.

449 The first compound is bryotoxin A, which could only be identified with exact  $m/z$   
450 matches in the MMCD database (Figure S6). While we collected an associated MS/MS  
451 spectrum, there were no corresponding listings in METLIN or MassBank which could help  
452 confirm the structure and identification. This compound is potentially interesting because it has  
453 not previously been observed in marine systems and studies on its toxicity are limited to  
454 experiments with cattle (McKenzie et al., 1987; McKenzie et al., 1989).

455 The second compound is a complex organic compound containing both iodine and  
456 chlorine. The putative elemental formula for this feature is  $C_{22}H_{22}Cl_2I_2N_2O_7$  and we observed the  
457 feature primarily in the intracellular metabolites (Fig. 5). We observed the  $m/z$  values of both  
458  $^{35}Cl$ - and  $^{37}Cl$ -isotopologues at the same retention time (Fig. S7), confirming the presence of  
459 chlorine. Macroalgae are the primary source of halogenated organic compounds in marine

460 ecosystems (Carpenter et al., 2000; Gschwend et al., 1985; Schall et al., 1994) and *T.*  
461 *pseudonana* releases CH<sub>3</sub>I, a simple organic halogenated compound (Hughes et al., 2006). Yet,  
462 while *T. pseudonana* assimilates both iodide and iodate (de la Cuesta and Manley, 2009), to our  
463 knowledge this is the first observation that *T. pseudonana* may produce a complex organic  
464 compound containing both iodine and chlorine. In marine systems, between 40 and 90% of all  
465 soluble iodine-containing compounds are organic compounds (Gilfedder et al., 2008; Lai et al.,  
466 2011; Wong and Cheng, 1998), which play an important role in chemical ecology (Vanellander  
467 et al., 2012) and marine atmospheric chemistry (O'Dowd et al., 2002; Saiz-Lopez et al., 2011).

468 We also observed over one hundred features that were tentatively identified as peptides  
469 (Table S3), mostly tripeptides (e.g., Arg-Tyr-Tyr) and a smaller number of dipeptides (e.g, Ala-  
470 Pro). Matches to *m/z* values in the METLIN database provide insight into the possible  
471 combinations of amino acids that compose the peptides we observed. However, peptide  
472 identification is challenging because (1) the amino acid sequence cannot be determined solely  
473 based on exact mass and (2) there are structural isomers among the twenty possible amino acids  
474 (He et al., 2004). While we will require additional analyses to identify the peptides we observed,  
475 the prevalence of *m/z* values matching peptides is noteworthy even without a putative  
476 identification of the amino acid sequences. The peptides were primarily present in the external  
477 metabolites, and were not always simultaneously present in the intracellular metabolite pool.  
478 Furthermore, plots of the peptides' EIC peak heights over time revealed statistically significant  
479 increases in peak heights (Pearson correlation coefficients with  $p < 0.05$ ) for the majority of the  
480 peptides (Table S3). This suggests that most of the peptides were increasing in concentration  
481 over the course of the experiment.

482           The unexpected observation of a large number of different peptides raises the question as  
483 to why *T. pseudonana* releases so many different peptides and whether the peptides would be  
484 readily assimilated by marine heterotrophic microorganisms. Free amino acids have been  
485 quantified inside and outside of the cells in *Skeletonema costatum* cultures and they represented a  
486 minor fraction (<5%) of the released dissolved organic carbon (Granum et al., 2002). More  
487 recently, a metabolomic investigation of *Synechococcus* revealed the presence of amino acids  
488 and dipeptides both inside the cells and in the growth media (Baran et al., 2010). Thus, the  
489 peptides we observe during *T. pseudonana* growth may be a product of protein turnover within  
490 the cell which is subsequently released into the media. Dissolved peptides are easily hydrolyzed  
491 to their constituent amino acids and then are rapidly consumed by heterotrophic microorganisms  
492 (Hollibaugh and Azam, 1983; Kirchman and Hodson, 1986). As a result, any peptides released  
493 by *T. pseudonana* are likely to have a short residence time in the marine environment. Further  
494 work is needed to assess whether the peptides observed here will be consumed at different rates  
495 depending on the carbon, nitrogen, and sulfur demands of the *in situ* heterotrophic bacterial  
496 community.

497           Metabolomics lags far behind other ‘omics’ investigations and, until recently,  
498 metabolomics research has focused on the development of laboratory methods, analytical  
499 methods, and computational tools. In the present project we applied these emerging tools to  
500 characterize the organic compounds that *T. pseudonana* may release into the environment.  
501 Through this analysis we putatively identified compounds not previously associated with *T.*  
502 *pseudonana* metabolism. While there have been only limited metabolomic investigations into the  
503 impact of marine microorganisms on their chemical environment, the continued development of

504 computational tools and establishment of new databases will be crucial in facilitating the  
505 comparison of metabolites across organisms and ecosystems.

## 506 **Acknowledgments**

507           We thank the people at [www.metabolomics-forum.com](http://www.metabolomics-forum.com) for answering questions about the  
508 use of XCMS and CAMERA, Matthew Monroe at PNNL for information about data file  
509 conversions, Erin Bertrand for discussions about the peptides, Paul Henderson for analyzing the  
510 nutrient samples, and Winn Johnson for information about the analysis of DMSP. Comments  
511 from the manuscript reviewers were much appreciated and helped clarify the presentation of the  
512 project. Instrumentation in the WHOI FT-MS facility was funded by the National Science  
513 Foundation MRI program (OCE-0619608) and by the Gordon and Betty T. Moore Foundation.  
514 This work was supported by NSF grant OCE-0928424 to EBK.

515



## 516 **Figure Legends**

517 Fig. 1. Extraction efficiency for the solid phase extraction of extracellular metabolites during the  
518 course of the experiment. The extraction efficiencies for the treatments with *T. pseudonana* is the  
519 percentage of the dissolved organic carbon retained by the PPL cartridges as a fraction of the  
520 measured dissolved organic carbon in the filtrate.

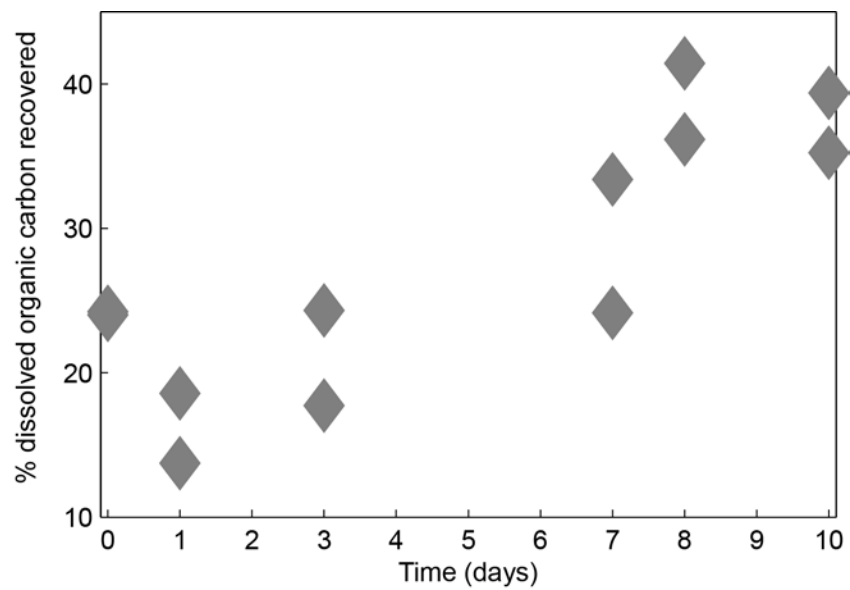
521 Fig. 2. The number of (A) protein-like, (B) condensed hydrocarbon-like, and (C) lipid-like  
522 compounds in the samples with *T. pseudonana* over the course of the experiment. The features  
523 within the cell-free controls were removed from the dataset prior to calculating the elemental  
524 formulas needed to define features based on their elemental ratios.

525 Fig. 3. NMS analysis based on presence or absence of features showing the differences in the  
526 composition of organic matter analyzed in (A and B) positive ion mode and (C and D) negative  
527 ion mode. The panels contain the same data coded differently to highlight (A and C) the  
528 differences between intracellular and extracellular metabolites or (B and D) the sampling time  
529 for the intracellular and extracellular metabolites.

530 Fig. 4. Changes in the (A) EIC peak height of a feature putatively identified as tri-N-  
531 acetylchitotriose. Data from both replicates with *T. pseudonana* are shown in the figure. The  
532 identification was based on  $m/z$  value and (B) comparison of the MS/MS spectrum with data  
533 available in METLIN. The structure of the compound is given within panel (A). The MS/MS  
534 spectrum shown in (B) is that from our unknown feature and the table lists the  $m/z$  values and  
535 relative intensities given in METLIN.

536 Fig. 5. The organic compound potentially containing both chlorine and iodine was (A) observed  
537 in negative ion mode as  $[M - 2H + Na]^-$ . The structure of the compound as shown in PubChem is  
538 given in (B).

539 Longnecker, Kido Soule, Kujawinski  
540 Fig. 1  
541



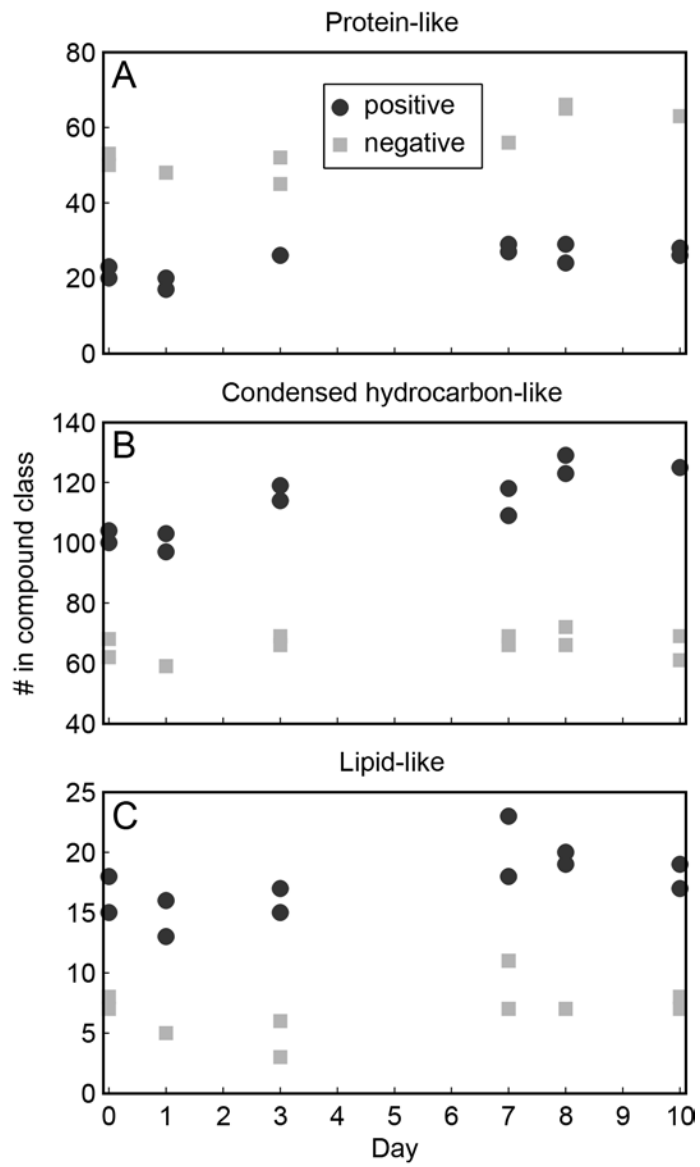


Fig. 3

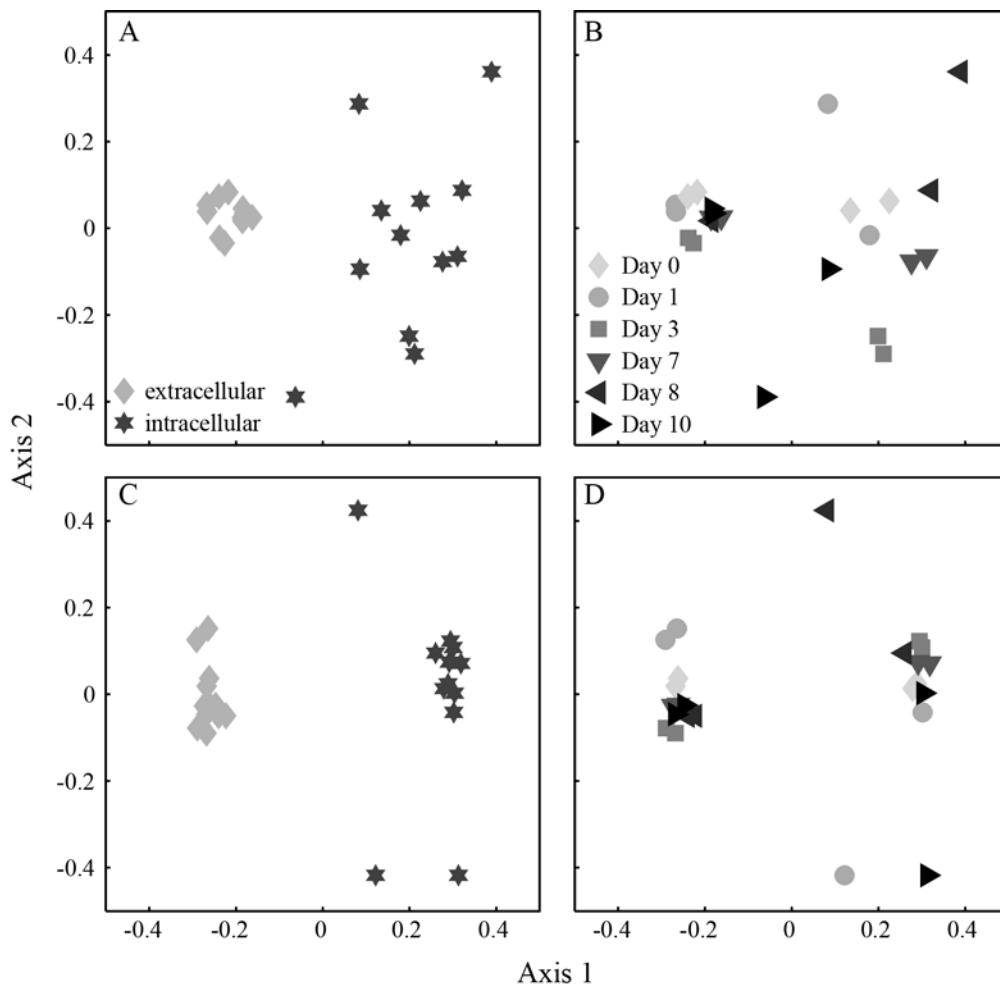
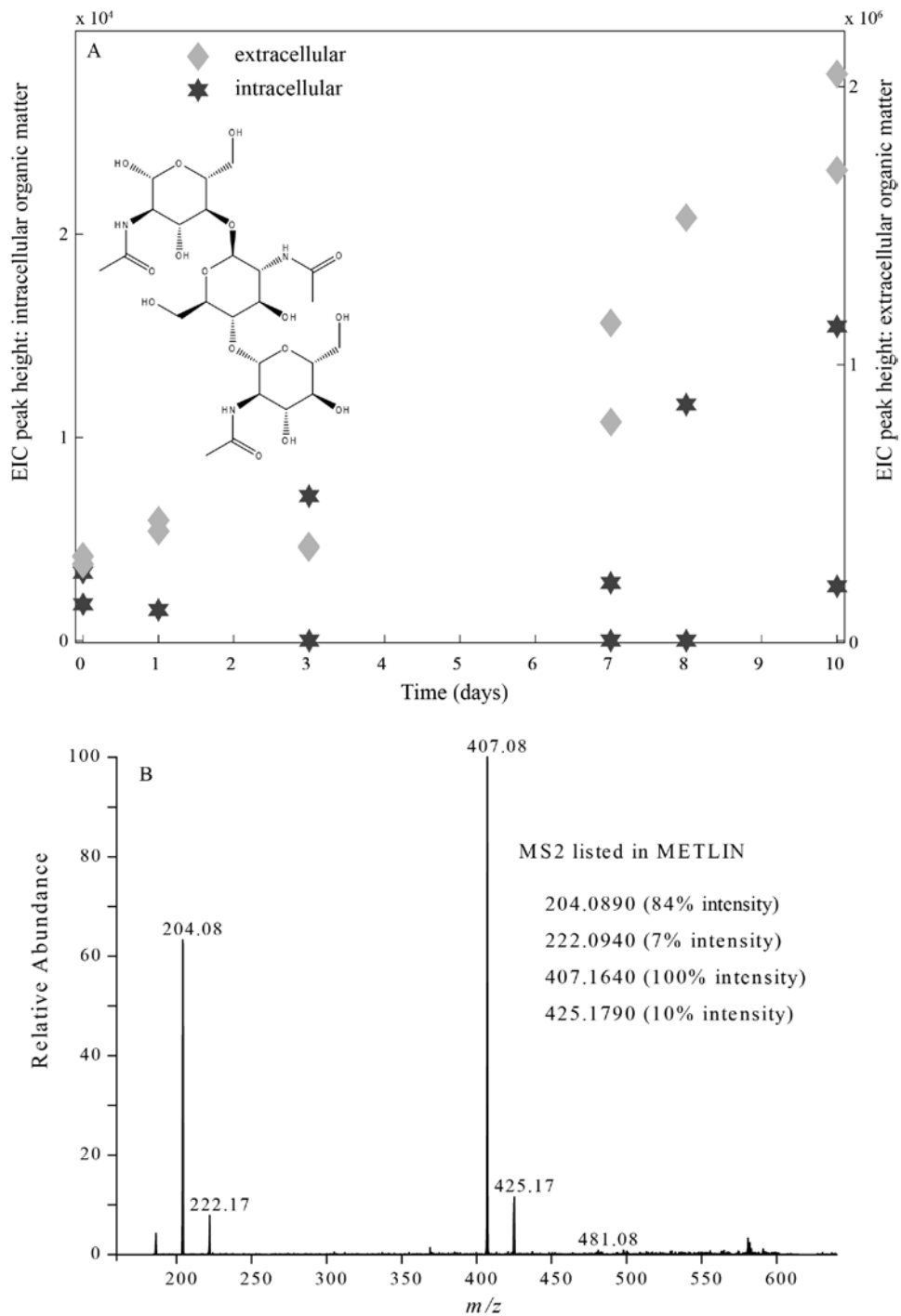


Fig. 4

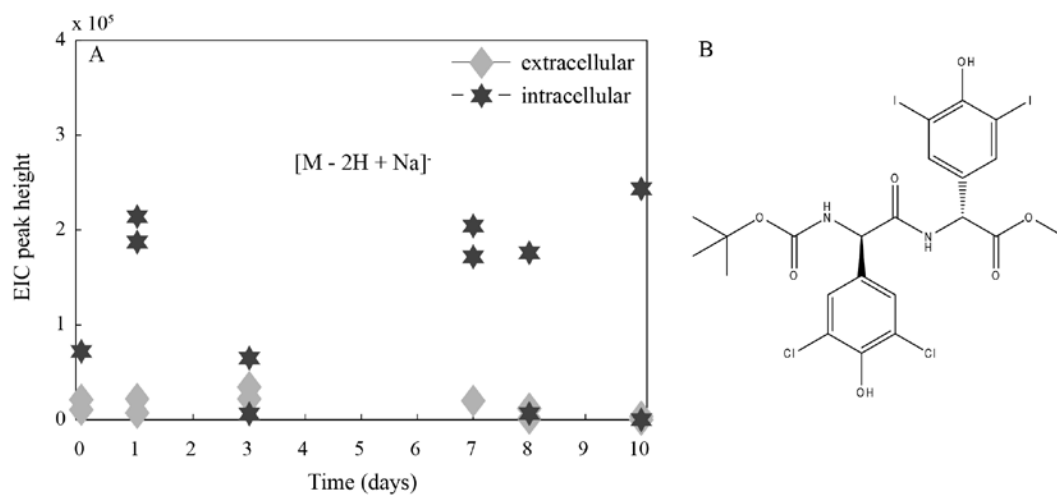


548  
549

Longnecker, Kido Soule, Kujawinski

550 Fig. 5

551  
552



553 Table 1. Summary of extracellular and intracellular metabolites exuded or retained by *T.*  
 554 *pseudonana*, as collected by LC/FT-MS in either positive or negative ion mode. Each feature is a  
 555 unique combination of an  $m/z$  value and a retention time.

	Negative	Positive
Total # of unique features	5484	12443
Number (and percent) of features remaining after deleting features found in the controls	4015 (73%)	9042 (73%)
# of features in the extracellular metabolites <sup>§</sup>	1630	2203
# of features in the intracellular metabolites <sup>§</sup>	1458	3685
# of features found in both the intracellular and extracellular metabolites <sup>†</sup>	9	35

556

557 <sup>§</sup>Features present in both replicates of either the extracellular or intracellular metabolites.

558 <sup>†</sup>Each feature had to be present in both replicates of the intracellular and extracellular metabolites  
 559 and present at more than one time point during the experiment.

560

561 Table 2. Details on the compounds putatively identified in the experiments with *T. pseudonana*.  
 562 The table includes the information on the measured  $m/z$  value and the ionization mode.  
 563 Additional details on each compound are presented in Table S2. Identification level is described  
 564 in the text and follows the convention proposed by Sumner et al. (2007).

<b>Putative annotation</b>	<b>Measured mass/charge</b>	<b>Ionization mode</b>	<b>Reference numbers</b>	<b>Identification level</b>
Tri-N-acetylchitotriose	628.255600	Positive	PubChem CID 444514	1
Chitobiose	425.176513	Positive	KEGG C01674	2
Dimethylsulfoniopropionate (DMSP)	135.047394	Positive	KEGG C04022	1
Bryotoxin A	619.275800	Positive	KEGG C08853	3
Organo-iodine compound	770.865479	Negative	PubChem CID 11535056	3

565

566



567 **References**

- 568 Armbrust, E.V., Berges, J.A., Bowler, C., Green, B.R., Martinez, D., Putnam, N.H. et al., The  
569 genome of the diatom *Thalassiosira pseudonana*: ecology, evolution, and metabolism. *Science*  
570 2004;306:79-86.
- 571 Azam, F. and Worden, A.Z., Microbes, molecules, and marine ecosystems. *Science*  
572 2004;303:1622-4.
- 573 Baran, R., Bowen, B.P., Bouskill, N.J., Brodie, E.L., Yannone, S.M. and Northen, T.R.,  
574 Metabolite identification in *Synechococcus* sp. PCC 7002 using untargeted stable isotope  
575 assisted metabolite profiling. *Anal Chem* 2010;82:9034-42.
- 576 Barofsky, A., Vidoudez, C. and Pohnert, G., Metabolic profiling reveals growth stage variability  
577 in diatom exudates. *Limnol Oceanogr Meth* 2009;7:382-90.
- 578 Becker, J.W., Berube, P.M., Follett, C.L., Waterbury, J.B., Chisholm, S.W., DeLong, E.F. et al.,  
579 Closely related phytoplankton species produce similar suites of dissolved organic matter.  
580 *Frontiers in Microbiology* 2014;5.
- 581 Bennette, N.B., Eng, J.F. and Dismukes, G.C., An LC-MS-based chemical and analytical method  
582 for targeted metabolite quantification in the model cyanobacterium *Synechococcus* sp. PCC  
583 7002. *Anal Chem* 2011;83:3808-16.
- 584 Bhatia, M.P., Das, S.B., Longnecker, K., Charette, M.A. and Kujawinski, E.B., Molecular  
585 characterization of dissolved organic matter associated with the Greenland ice sheet *Geochim*  
586 *Cosmochim Acta* 2010;74:3768-84.
- 587 Böttcher, C., Edda von, R.-L., Schmidt, J., Schmotz, C., Neumann, S., Scheel, D. et al.,  
588 Metabolome analysis of biosynthetic mutants reveals a diversity of metabolic changes and allows  
589 identification of a large number of new compounds in *Arabidopsis*. *Plant Physiology*  
590 2008;147:2107-20.
- 591 Bowler, C., Vardi, A. and Allen, A.E., Oceanographic and biogeochemical insights from diatom  
592 genomes. *Annu Rev Mar Sci* 2010;2:333-65.
- 593 Bromke, M.A., Giavalisco, P., Willmitzer, L. and Hesse, H., Metabolic analysis of adaptation to  
594 short-term changes in culture conditions of the marine diatom *Thalassiosira pseudonana*. *PLoS*  
595 *ONE* 2013;8.
- 596 Brunner, E., Richthammer, P., Ehrlich, H., Paasch, S., Simon, P., Ueberlein, S. et al., Chitin-  
597 based organic networks: an integral part of cell wall biosilica in the diatom *Thalassiosira*  
598 *pseudonana*. *Angew Chem Int Ed* 2009;48:9724-7.
- 599 Bucciarelli, E. and Sunda, W.G., Influence of CO<sub>2</sub>, nitrate, phosphate, and silicate limitation on  
600 intracellular dimethylsulfoniopropionate in batch cultures of the coastal diatom *Thalassiosira*  
601 *pseudonana*. *Limnol Oceanogr* 2003;48:2256-65.

602 Carlson, C.A., 2002. Production and removal processes. In: D.A. Hansell and C.A. Carlson  
603 (Editors), Biogeochemistry of marine dissolved organic matter. Academic Press, pp. 91-151.

604 Carpenter, L.J., Malin, G., Liss, P.S. and Kupper, F.C., Novel biogenic iodine-containing  
605 trihalomethanes and other short-lived halocarbons in the coastal East Atlantic. Global  
606 Biogeochem Cy 2000;14:1191-204.

607 Chambers, M.C., Maclean, B., Burke, R., Amodei, D., Ruderman, D.L., Neumann, S. et al., A  
608 cross-platform toolkit for mass spectrometry and proteomics. Nat Biotech 2012;30:918-20.

609 Cui, Q., Lewis, I.A., Hegeman, A.D., Anderson, M.E., Li, J., Schulte, C.F. et al., Metabolite  
610 identification via the Madison Metabolomics Consortium Database. Nat Biotech 2008;26:162-4.

611 Daly, R., Rogers, S., Wandy, J., Jankevics, A., Burgess, K.E.V. and Breitling, R., MetAssign:  
612 probabilistic annotation of metabolites from LC-MS data using a Bayesian clustering approach.  
613 Bioinformatics 2014.

614 de la Cuesta, J.L. and Manley, S.L., Iodine assimilation by marine diatoms and other  
615 phytoplankton in nitrate-replete conditions. Limnol Oceanogr 2009;54:1653-64.

616 del Giorgio, P.A. and Cole, J.J., Bacterial growth efficiency in natural aquatic systems. Annu  
617 Rev Ecol Syst 1998;29:503-41.

618 Dittmar, T., Koch, B., Hertkorn, N. and Kattner, G., A simple and efficient method for the solid-  
619 phase extraction of dissolved organic matter (SPE-DOM) from seawater. Limnol Oceanogr Meth  
620 2008;6:230-5.

621 Dunn, W.B., Broadhurst, D., Begley, P., Zelena, E., Francis-McIntyre, S., Anderson, N. et al.,  
622 Procedures for large-scale metabolic profiling of serum and plasma using gas chromatography  
623 and liquid chromatography coupled to mass spectrometry. Nat Protocols 2011;6:1060-83.

624 Durkin, C.A., Mock, T. and Armbrust, E.V., Chitin in diatoms and its association with the cell  
625 wall. Eukaryot Cell 2009;EC.00079-09.

626 Dyhrman, S.T., Jenkins, B.D., Rynearson, T.A., Saito, M.A., Mercier, M.L., Alexander, H. et al.,  
627 The transcriptome and proteome of the diatom *Thalassiosira pseudonana* reveal a diverse  
628 phosphorus stress response. PLoS ONE 2012;7:e33768.

629 Franklin, D.J., Airs, R.L., Fernandes, M., Bell, T.G., Bongaerts, R.J., Berges, J.A. et al.,  
630 Identification of senescence and death in *Emiliania huxleyi* and *Thalassiosira pseudonana*: Cell  
631 staining, chlorophyll alterations, and dimethylsulphoniopropionate (DMSP) metabolism. Limnol  
632 Oceanogr 2012;57:305-17.

633 Gilfedder, B.S., Lai, S.C., Petri, M., Biester, H. and Hoffmann, T., Iodine speciation in rain,  
634 snow and aerosols. Atmos Chem Phys 2008;8:6069-84.

- 635 Gooday, G.W., 1990. The ecology of chitin degradation. In: K.C. Marshall, R.M. Atlas, J.G.  
636 Jones and B.B. Jorgensen (Editors), *Adv Microb Ecol*. Plenum, New York, New York, pp. 387-  
637 430.
- 638 Granum, E., Kirkvold, S. and Myklestad, S.M., Cellular and extracellular production of  
639 carbohydrates and amino acids by the marine diatom *Skeletonema costatum*: diel variations and  
640 effects of N depletion. *Mar Ecol Prog Ser* 2002;242:83-94.
- 641 Gschwend, P.M., Macfarlane, J.K. and Newman, K.A., Volatile halogenated organic compounds  
642 released to seawater from temperate marine macroalgae. *Science* 1985;227:1033-5.
- 643 He, F., Emmett, M.R., Håkansson, K., Hendrickson, C.L. and Marshall, A.G., Theoretical and  
644 experimental prospects for protein identification based solely on accurate mass measurement. *J*  
645 *Proteome Res* 2004;3:61-7.
- 646 Hedges, J.I., 1990. Compositional indicators of organic acid sources and reactions in natural  
647 environments. In: E.M. Perdue and E.T. Gjessing (Editors), *Organic Acids in Aquatic*  
648 *Ecosystems*. John Wiley & Sons Ltd.
- 649 Hildebrand, M., Kim, S., Shi, D., Scott, K. and Subramaniam, S., 3D imaging of diatoms with  
650 ion-abrasion scanning electron microscopy. *J Struct Biol* 2009;166:316-28.
- 651 Hollibaugh, J.T. and Azam, F., Microbial degradation of dissolved proteins in seawater. *Limnol*  
652 *Oceanogr* 1983;28:1104-16.
- 653 Horai, H., Arita, M., Kanaya, S., Nihei, Y., Ikeda, T., Suwa, K. et al., MassBank: a public  
654 repository for sharing mass spectral data for life sciences. *J Mass Spectrom* 2010;45:703-14.
- 655 Hughes, C., Malin, G., Nightingale, P.D. and Liss, P.S., The effect of light stress on the release  
656 of volatile iodocarbons by three species of marine microalgae. *Limnol Oceanogr* 2006;51:2849-  
657 54.
- 658 Iijima, Y., Nakamura, Y., Ogata, Y., Tanaka, K., Sakurai, N., Suzuki, T. et al., Metabolite  
659 annotations based on the integration of mass spectral information. *Plant J* 2008;54:949 - 62.
- 660 Jeuniaux, C. and Voss-Foucart, M.F.o., Chitin biomass and production in the marine  
661 environment. *Biochem Syst Ecol* 1991;19:347-56.
- 662 Keller, M.D., Kiene, R.P., Matrai, P.A. and Bellows, W.K., Production of glycine betaine and  
663 dimethylsulfoniopropionate in marine phytoplankton. II. N-limited chemostat cultures. *Mar Biol*  
664 1999;135:249-57.
- 665 Kim, S., Kramer, R.W. and Hatcher, P.G., Graphical method for analysis of ultrahigh-resolution  
666 broadband mass spectra of natural organic matter, the van krevelen diagram. *Anal Chem*  
667 2003;75:5336-44.
- 668 Kind, T., Scholz, M. and Fiehn, O., How large is the metabolome? A critical analysis of data  
669 exchange practices in chemistry. *PLoS ONE* 2009;4:e5440.

- 670 Kirchman, D.L., 2008. Introduction and Overview. In: D.L. Kirchman (Editor), Microbial  
671 Ecology of the Oceans. Wiley-Blackwell, pp. 1-44.
- 672 Kirchman, D.L. and Hodson, R.E., Metabolic regulation of amino acid uptake in marine waters.  
673 Limnol Oceanogr 1986;31:339-50.
- 674 Kirst, G.O., Salinity tolerance of eukaryotic marine algae. Annu Rev Plant Phys 1990;41:21-53.
- 675 Kruskal, J.B., Multidimensional scaling by optimizing goodness of fit to a nonmetric hypothesis.  
676 Psychometrika 1964;29:1-27.
- 677 Kuhl, C., Tautenhahn, R., Böttcher, C., Larson, T.R. and Neumann, S., CAMERA: an integrated  
678 strategy for compound spectra extraction and annotation of liquid chromatography/mass  
679 spectrometry data sets. Anal Chem 2012;84:283-9.
- 680 Kujawinski, E.B., The impact of microbial metabolism on marine dissolved organic matter.  
681 Annu Rev Mar Sci 2011;3:567-99.
- 682 Kujawinski, E.B. and Behn, M.D., Automated analysis of electrospray ionization Fourier-  
683 transform ion cyclotron resonance mass spectra of natural organic matter. Anal Chem  
684 2006;78:4363-73.
- 685 Kujawinski, E.B., Longnecker, K., Blough, N.V., Del Vecchio, R., Finlay, L., Kitner, J.B. et al.,  
686 Identification of possible source markers in marine dissolved organic matter using ultrahigh  
687 resolution mass spectrometry. Geochim Cosmochim Acta 2009;73:4384-99.
- 688 Lai, S.C., Williams, J., Arnold, S.R., Atlas, E.L., Gebhardt, S. and Hoffmann, T., Iodine  
689 containing species in the remote marine boundary layer: The link to oceanic phytoplankton.  
690 Geophys Res Lett 2011;38:L20801.
- 691 Long, J.Z., Cisar, J.S., Milliken, D., Niessen, S., Wang, C., Trauger, S.A. et al., Metabolomics  
692 annotates ABHD3 as a physiologic regulator of medium-chain phospholipids. Nature chemical  
693 biology 2011;7:763-5.
- 694 Longnecker, K. and Kujawinski, E.B., Composition of dissolved organic matter in groundwater.  
695 Geochim Cosmochim Acta 2011;75:2752-61.
- 696 Mather, P.M., 1976. Computational methods of multivariate analysis in physical geography. J.  
697 Wiley & Sons, London, 532 pp.
- 698 McKenzie, R.A., Franke, F.P. and Dunster, P.J., The toxicity to cattle and bufadienolide content  
699 of six *Bryophyllum* species. Aust Vet J 1987;64:298-301.
- 700 McKenzie, R.A., Franke, F.P. and Dunster, P.J., The toxicity for cattle of bufadienolide cardiac  
701 glycosides from *Bryophyllum tubiflorum* flowers. Aust Vet J 1989;66:374-6.

702 Minor, E.C., Steinbring, C.J., Longnecker, K. and Kujawinski, E.B., Characterization of  
703 dissolved organic matter in Lake Superior and its watershed using ultrahigh resolution mass  
704 spectrometry. *Org Geochem* 2012;43:1-11.

705 Montsant, A., Allen, A.E., Coesel, S., Martino, A.D., Falciatore, A., Mangogna, M. et al.,  
706 Identification and comparative genomic analysis of signaling and regulatory components in the  
707 diatom *Thalassiosira pseudonana*. *J Phycol* 2007;43:585-604.

708 Nelson, D.M., Treguer, P., Brzezinski, M.A., Leynaert, A. and Queguiner, B., Production and  
709 dissolution of biogenic silica in the ocean - revised global estimates, comparison with regional  
710 data and relationship to biogenic sedimentation. *Global Biogeochem Cy* 1995;9:359-72.

711 Norden-Krichmar, T.M., Allen, A.E., Gaasterland, T. and Hildebrand, M., Characterization of  
712 the small RNA transcriptome of the diatom, *Thalassiosira pseudonana*. *PLoS ONE*  
713 2011;6:e22870.

714 Nunn, B.L., Aker, J.R., Shaffer, S.A., Tsai, Y.H., Strzeppek, R.F., Boyd, P.W. et al., Deciphering  
715 diatom biochemical pathways via whole-cell proteomics. *Aquat Microb Ecol* 2009;55:241-53.

716 O'Dowd, C.D., Jimenez, J.L., Bahreini, R., Flagan, R.C., Seinfeld, J.H., Hämeri, K. et al., Marine  
717 aerosol formation from biogenic iodine emissions. *Nature* 2002;417:632-6.

718 Patti, G.J., Yanes, O. and Siuzdak, G., Metabolomics: the apogee of the omics trilogy. *Nat Rev*  
719 *Mol Cell Bio* 2012;13:263-9.

720 Paul, C., Barofsky, A., Vidoudez, C. and Pohnert, G., Diatom exudates influence metabolism and  
721 cell growth of co-cultured diatom species. *Mar Ecol Prog Ser* 2009;389:61-70.

722 Quanbeck, S.M.M., Brachova, L., Campbell, A.A., Guan, X., Perera, A., He, K. et al.,  
723 Metabolomics as a hypothesis-generating functional genomics tool for the annotation of  
724 *Arabidopsis thaliana* genes of "unknown function". *Frontiers in Plant Science* 2012;3.

725 Rabinowitz, J.D. and Kimball, E., Acidic acetonitrile for cellular metabolome extraction from  
726 *Escherichia coli*. *Anal Chem* 2007;79:6167-73.

727 Romano, S., Dittmar, T., Bondarev, V., Weber, R.J.M., Viant, M.R. and Schulz-Vogt, H.N.,  
728 Exo-metabolome of *Pseudovibrio* sp. FO-BEG1 analyzed by ultra-high resolution mass  
729 spectrometry and the effect of phosphate limitation. *PLoS ONE* 2014;9:e96038.

730 Rosselló-Mora, R., Lucio, M., Peña, A., Brito-Echeverría, J., López-López, A., Valens-Vadell,  
731 M. et al., Metabolic evidence for biogeographic isolation of the extremophilic bacterium  
732 *Salinibacter ruber*. *ISME J* 2008;2:242-53.

733 Saiz-Lopez, A., Plane, J.M.C., Baker, A.R., Carpenter, L.J., von Glasow, R., Gómez Martín, J.C.  
734 et al., Atmospheric chemistry of iodine. *Chem Rev* 2011.

735 Schall, C., Laturus, F. and Heumann, K.G., Biogenic volatile organoiodine and organobromine  
736 compounds released from polar macroalgae. *Chemosphere* 1994;28:1315-24.

- 737 Schymanski, E. and Neumann, S., The Critical Assessment of Small Molecule Identification  
738 (CASMI): challenges and solutions. *Metabolites* 2013;3:517-38.
- 739 Shi, X., Gao, W., Chao, S.-h., Zhang, W. and Meldrum, D.R., Monitoring the single-cell stress  
740 response of the diatom *Thalassiosira pseudonana* by quantitative real-time reverse transcription-  
741 PCR. *Appl Environ Microbiol* 2013;79:1850-8.
- 742 Smith, C.A., O'Maille, G., Want, E.J., Qin, C., Trauger, S.A., Brandon, T.R. et al., 2005.  
743 METLIN: A Metabolite Mass Spectral Database 9th International Congress of Therapeutic Drug  
744 Monitoring and Clinical Toxicology, Louisville, Kentucky.
- 745 Smith, C.A., Want, E.J., O'Maille, G., Abagyan, R. and Siuzdak, G., XCMS: processing mass  
746 spectrometry data for metabolite profiling using nonlinear peak alignment, matching, and  
747 identification. *Anal Chem* 2006;78:779 - 87.
- 748 Smucker, R.A. and Dawson, R., Products of photosynthesis by marine phytoplankton: Chitin in  
749 TCA "protein" precipitates. *J Exp Mar Biol Ecol* 1986;104:143-52.
- 750 Stefels, J., Steinke, M., Turner, S., Malin, G. and Belviso, S., Environmental constraints on the  
751 production and removal of the climatically active gas dimethylsulphide (DMS) and implications  
752 for ecosystem modelling. *Biogeochemistry* 2007;83:245-75.
- 753 Štrojsová, A. and Dyhrman, S.T., Cell-specific  $\beta$ -N-acetylglucosaminidase activity in cultures  
754 and field populations of eukaryotic marine phytoplankton. *FEMS Microbiol Ecol* 2008;64:351-  
755 61.
- 756 Suhre, K. and Schmitt-Kopplin, P., MassTRIX: mass translator into pathways. *Nucleic Acids*  
757 *Res* 2008;36:W481-4.
- 758 Sumner, L., Amberg, A., Barrett, D., Beale, M., Beger, R., Daykin, C. et al., Proposed minimum  
759 reporting standards for chemical analysis. *Metabolomics* 2007;3:211-21.
- 760 Tautenhahn, R., Bottcher, C. and Neumann, S., Highly sensitive feature detection for high  
761 resolution LC/MS. *BMC Bioinformatics* 2008;9:504.
- 762 Tréguer, P., Nelson, D.M., Bennekom, A.J.V., DeMaster, D.J., Leynaert, A. and Quéguiner, B.,  
763 The silica balance in the world ocean: a reestimate. *Science* 1995;268:375-9.
- 764 Vanellander, B., Paul, C., Grueneberg, J., Prince, E.K., Gillard, J., Sabbe, K. et al., Daily bursts  
765 of biogenic cyanogen bromide (BrCN) control biofilm formation around a marine benthic  
766 diatom. *Proc Natl Acad Sci USA* 2012.
- 767 Vidoudez, C. and Pohnert, G., Comparative metabolomics of the diatom *Skeletonema marinoi* in  
768 different growth phases. *Metabolomics* 2012;8:654-69.
- 769 Winder, C.L., Dunn, W.B., Schuler, S., Broadhurst, D., Jarvis, R., Stephens, G.M. et al., Global  
770 metabolic profiling of *Escherichia coli* cultures: an evaluation of methods for quenching and  
771 extraction of intracellular metabolites. *Anal Chem* 2008;80:2939-48.

772 Wong, G.T.F. and Cheng, X.-H., Dissolved organic iodine in marine waters: Determination,  
773 occurrence and analytical implications. Mar Chem 1998;59:271-81.  
774  
775

## **Dissolved organic matter produced by *Thalassiosira pseudonana***

Supporting Information

Krista Longnecker, Melissa C. Kido Soule, and Elizabeth B. Kujawinski\*.

Woods Hole Oceanographic Institution, Marine Chemistry and Geochemistry, Woods Hole, MA  
02543, U.S.A.

TITLE RUNNING HEAD: Phytoplankton metabolomics

\*Corresponding author. Mailing address: WHOI MS#4, Woods Hole, MA 02543. Phone: (508)  
289-3493. Fax: (508) 457-2164. E-mail: ekujawinski@whoi.edu



Table S1. Percent of features with changes in EIC peak heights over time for features found in the samples and absent from the cell-free controls. Only statistically-significant (Model I regressions with  $p \leq 0.05$ ) increases or decreases are included in the table. The total # of features is also shown in Table 1 and is the number of features present in both replicates of either the extracellular or intracellular metabolite samples and absent from the cell-free controls.

	Positive		Negative	
	Intracellular	Extracellular	Intracellular	Extracellular
% features increased	4%	67%	5%	25%
% features decreased	7%	13%	6%	8%
Total # features	3685	2203	1458	1630

Table S2. Summary of the features of interest which could be putatively identified. The table indicates whether the features were detected in positive (pos) or negative (neg) ion mode, and what charged ion was detected. Error indicates the absolute difference between the observed  $m/z$  value and the calculated  $m/z$  value. MS/MS spectra were available for some of the features, and the comments include additional information about each feature. Reference numbers can be used to find additional information about each compound in the indicated database.

Putative annotation	Elemental Formula (exact mass)	Ion mode	Detected as?	Error (ppm)	MS/MS ?	Reference numbers	Comments
Tri-N-acetylchitotriose	C <sub>24</sub> H <sub>41</sub> N <sub>3</sub> O <sub>16</sub> (627.248682)	Pos	[M+H] <sup>+</sup>	0.57	Yes	PubChem CID 444514	1 match at METLIN with MS/MS data corresponding to the observed MS/MS data
Chitobiose	C <sub>16</sub> H <sub>28</sub> N <sub>2</sub> O <sub>11</sub> (424.169310)	Pos	[M+H] <sup>+</sup>	0.17	No	KEGG C01674	Same retention time as tri-N-acetylchitotriose
Dimethylsulfoniopropionate (DMSP)	C <sub>5</sub> H <sub>10</sub> O <sub>2</sub> S (134.040150)	Pos	[M+H] <sup>+</sup>	0.24	Yes	KEGG C04022	1 match at MMCD; no match at METLIN
Bryotoxin A	C <sub>32</sub> H <sub>42</sub> O <sub>12</sub> (618.267627)	Pos	[M+H] <sup>+</sup>	1.45	No	KEGG C08853	1 match at MMCD; no match at METLIN
Organo-iodine compound*	C <sub>22</sub> H <sub>22</sub> Cl <sub>2</sub> I <sub>2</sub> N <sub>2</sub> O <sub>7</sub> (749.889361)	Neg	[M-2H+Na] <sup>-</sup>	1.88	No	PubChem CID 11535056	No matches at MMCD or METLIN; found isotopes for <sup>37</sup> Cl

\* The full name for the organo-iodine compound is: Methyl (2R)-2-[[[(2R)-2-(3,5-dichloro-4-hydroxyphenyl)-2-[(2-methylpropan-2-yl)oxycarbonylamino]acetyl]amino]-2-(4-hydroxy-3,5-diiodophenyl)acetate

Table S3. Summary of peptide data from the intracellular and extracellular metabolites analyzed in positive or negative ion mode. Both dipeptides and tripeptides were observed. Most of the peptides showed increases in EIC peak heights over the course of the experiment.

	<b>Positive</b>		<b>Negative</b>	
	<b>Intracellular</b>	<b>Extracellular</b>	<b>Intracellular</b>	<b>Extracellular</b>
Total # of peptide matches	11	88	2	26
# compounds increased during experiment	6	68	2	23
# compounds decreased during experiment	5	20	0	3

Fig. S1. We used a mixture of metabolites to optimize the LC/FT-ICR-MS parameters. This solution consisted of L-methionine, L-proline, L-arginine, L-glutamic acid, L-glutamine, L-threonine, caffeine, n-acetyl D-glucosamine, riboflavin, biotin, thymidine, NAD, succinic acid, malic acid, orotic acid, phosphoenolpyruvate, citric acid, glucose 6-phosphate, fructose 1,6-bisphosphate, and sodium taurocholate. The total ion chromatograph is shown for (A) the analysis of the metabolite mix and a solvent blank (90:10 water:acetonitrile) in negative ion mode, (B) the analysis of the metabolite mixture and a solvent blank in positive ion mode. The text lists the metabolites (and retention time, in seconds) for each ionization mode.

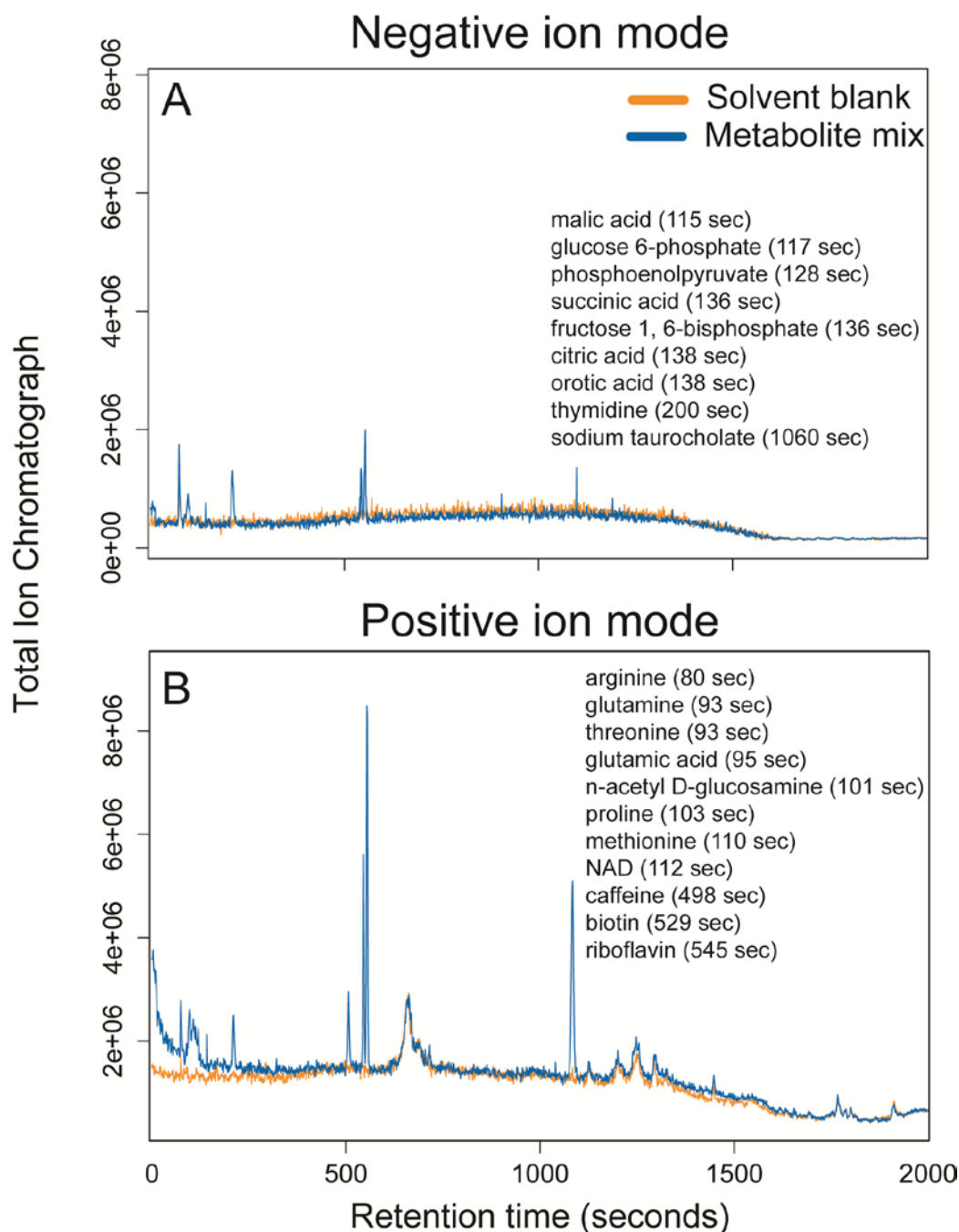


Fig. S2. During the incubation period, there were increases in (A) the abundance of *T. pseudonana* and (B) the concentration of total organic carbon within the flasks. There were no changes in the cell-free controls over the experiment, nor was there evidence of contamination by heterotrophic bacterial cells. The approximately 200  $\mu\text{M}$  of total organic carbon in the cell-free controls is due to the presence of vitamins and EDTA that are required by *T. pseudonana* for cell growth. (C) There was a decrease in the concentration of nitrate+nitrite in the flasks with *T. pseudonana* indicating the consumption of inorganic nutrients concurrent with increases in cellular abundance. Silicate and phosphate showed similar patterns in concentration (data not shown).

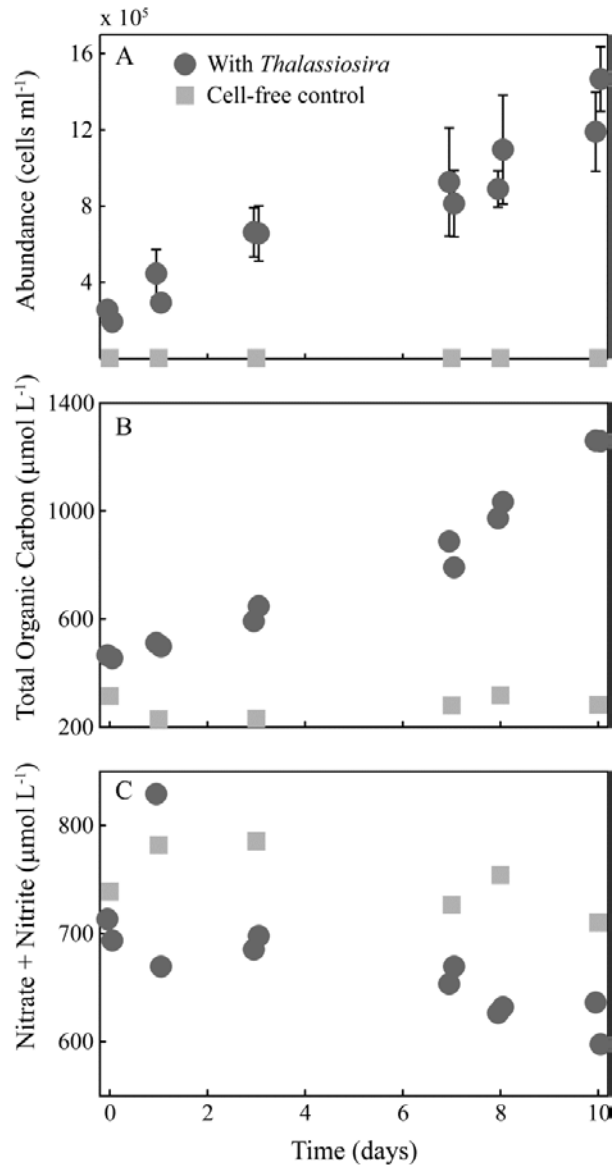


Fig. S3. The number of features (unique combinations of  $m/z$  value and retention time) for the extracellular and intracellular metabolites during the experiment from (A) positive ion mode and (B) negative ion mode. The points have been jiggered on the time axis to reduce overlap between sample points. A low number of features was observed in one of the extracellular metabolite samples at day 8 within the positive ion mode data. Inspection of the raw data revealed a problem with sample injection and this sample was not considered further.

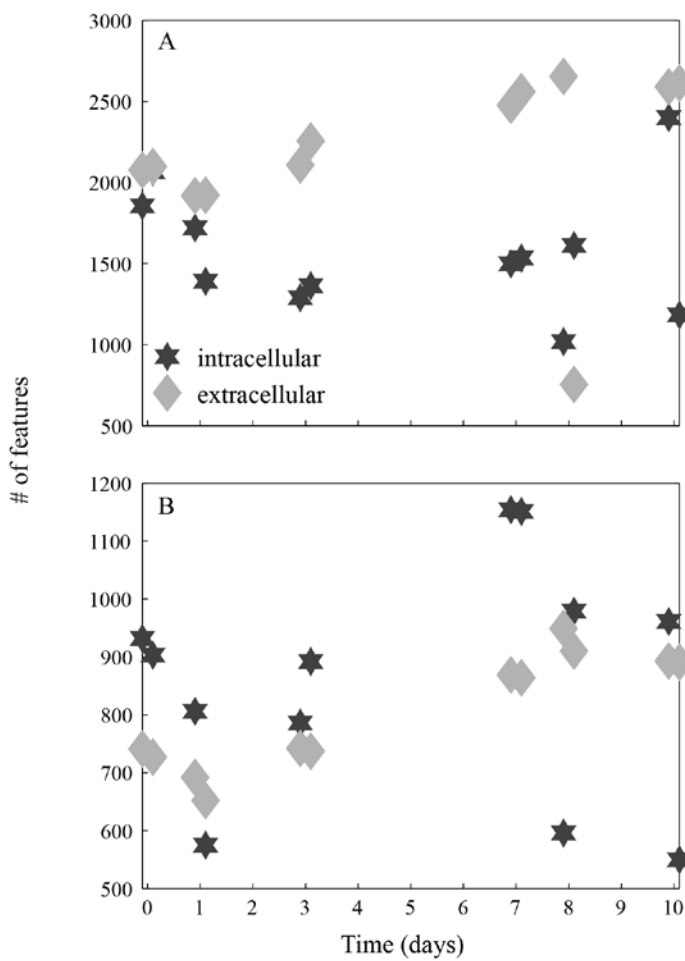


Fig. S4 : Extracted ion chromatogram (EIC) for tri-N-acetylchitotriose which had a measured  $m/z$  value of 628.52260. XCMS was used to process the data files generated by the LC-FT system. The dark lines are from samples with *T. pseudonana* while the lighter lines are the cell-free controls.

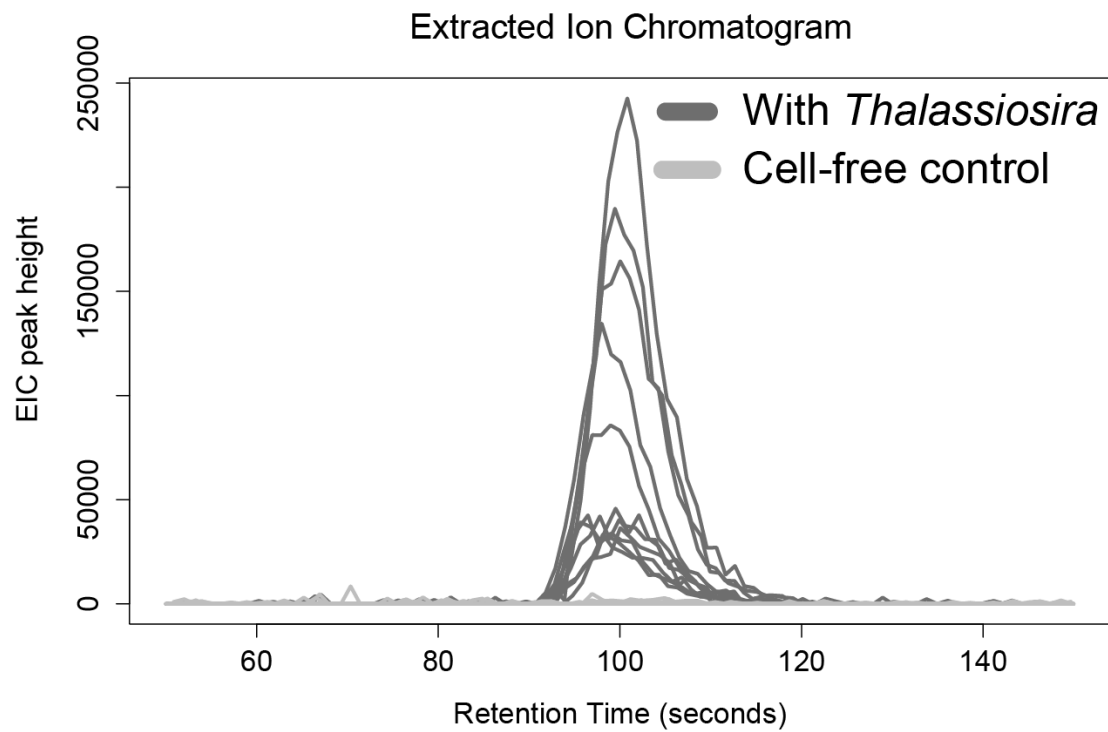




Fig. S5. DMSP was putatively identified in positive ion mode in both the intracellular and extracellular metabolites. The analysis failed for one of the replicates on day 8, and that sample is not plotted on the figure. Note the scale difference in the EIC peak heights between the intracellular and extracellular metabolites. The structure of the compound is also shown.

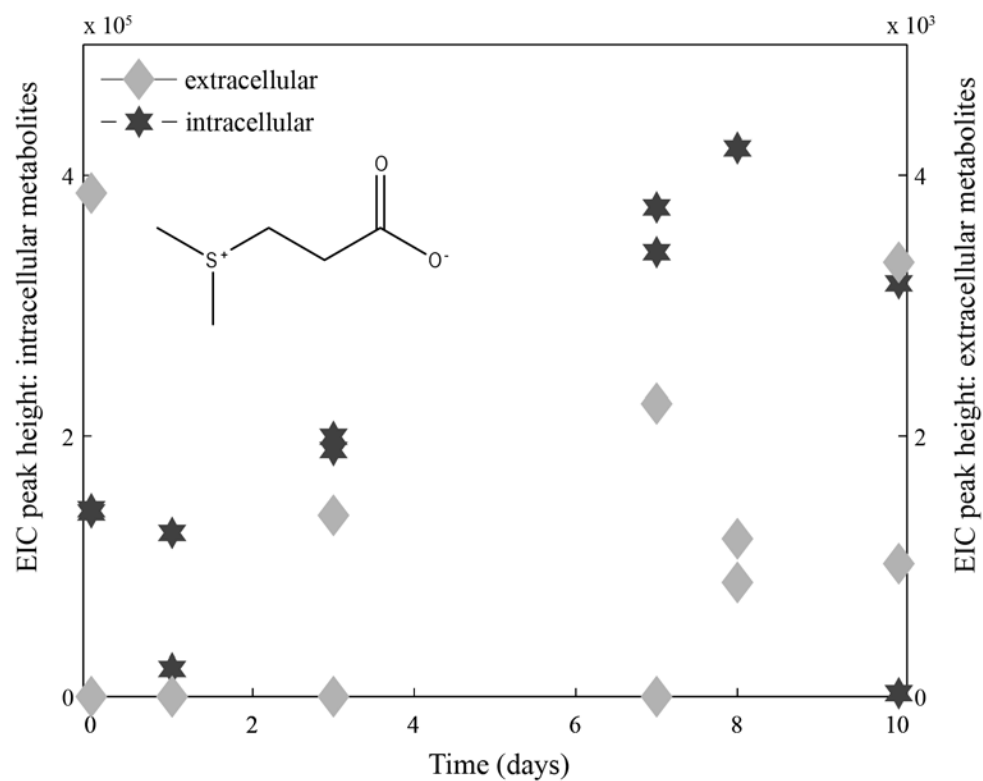


Fig. S6. A feature putatively annotated as bryotoxin A was observed in positive ion mode in both the intracellular and extracellular metabolites. Note the scale difference in the EIC peak heights between the intracellular and extracellular metabolites. The inset shows the structure of bryotoxin A, and the changes in EIC peak heights over the course of the experiment.

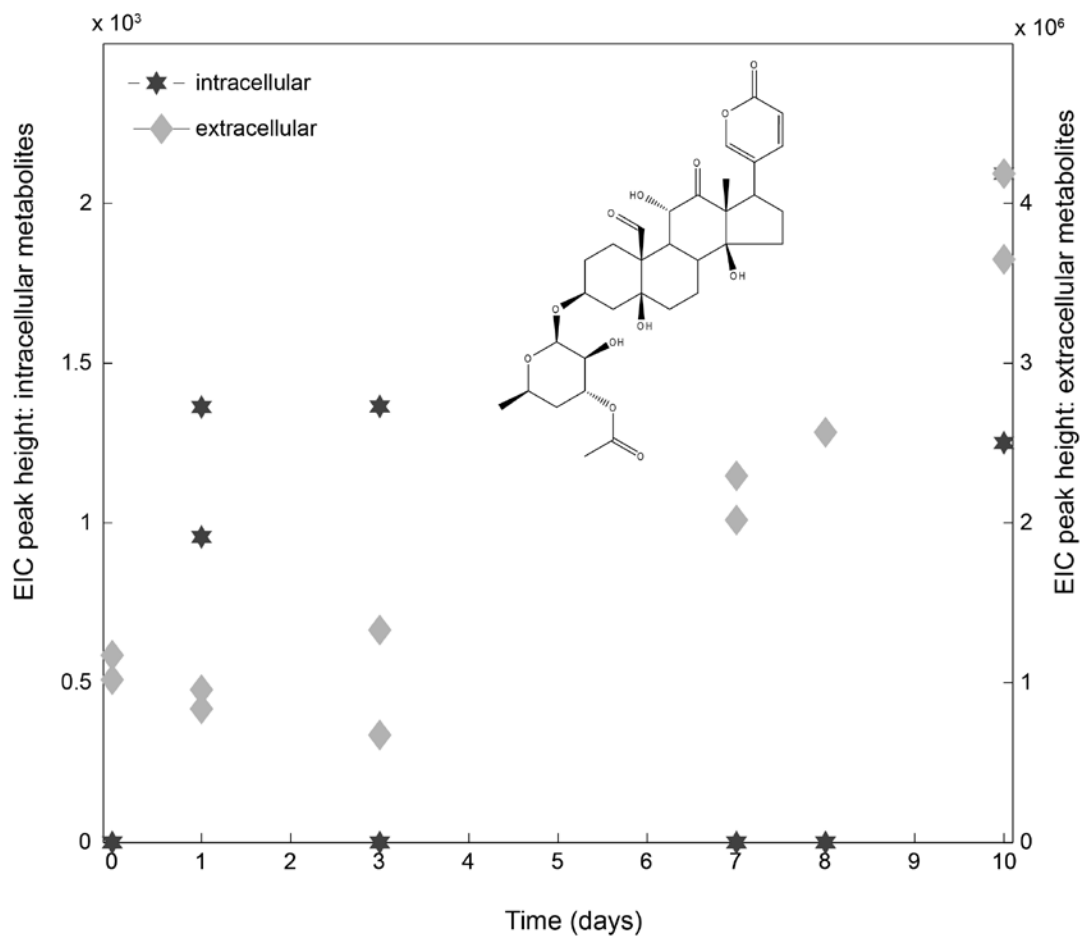


Fig. S7. EIC data for the organo-iodine compound ( $C_{22}H_{22}Cl_2I_2N_2O_7$ ) observed in negative ion mode at (A) day zero and (B) day ten of the experiment. The data in green show the compound with two  $^{35}Cl$  molecules, while the data in orange is the EIC data for a feature that putatively has one  $^{35}Cl$  and one  $^{37}Cl$ . In the environment, chlorine molecules are 75%  $^{35}Cl$  and 25%  $^{37}Cl$ , and our data show the  $^{35}Cl$  organo-iodine compound had higher EIC peak heights supporting our putative identification of a compound containing chlorine.

